ELSEVIER

Journal of Alloys and Compounds 446–447 (2007) 409–414

Journal of ALLOYS AND COMPOUNDS

www.elsevier.com/locate/jallcom

Thermodynamic destabilization and reaction kinetics in light metal hydride systems

John J. Vajo*, Tina T. Salguero, Adam F. Gross, Sky L. Skeith, Gregory L. Olson

HRL Laboratories, LLC, 3011 Malibu Canyon Road, Malibu, CA 90265, United States

Received 26 September 2006; received in revised form 2 February 2007; accepted 13 February 2007
Available online 20 February 2007

Abstract

Experimental approaches for altering the thermodynamics and kinetics of light element hydride systems are discussed. Equilibrium hydrogen pressures and reaction enthalpies can be varied with additives that form new alloy or compound phases upon dehydrogenation. The formation of new phases lowers the dehydrogenated state enthalpy and effectively destabilizes the component hydrides. This strategy is illustrated for $LiBH_4$ destabilized by MgH_2, MgF_2, MgS, and MgSe. The slow rates of hydrogen exchange in light element hydrides can be improved with catalysts and by reducing diffusion distances to the nanometer scale. The catalytic effects of a variety of transition metal sources on hydrogen exchange in the $LiBH_4/MgH_2$ system are described. The effects of reduced diffusion distances are illustrated using $LiBH_4$ incorporated into a nanoporous carbon aerogel.

Keywords: Hydrogen absorbing materials; Metal hydrides; Nanostructured materials; Catalysts

1. Introduction

The effective thermodynamic stability of a solid-state hydride (more generally, any chemical compound) depends strongly on its chemical environment. A simple example is methane, which in isolation is thermodynamically stable, i.e., the dissociation of methane into molecular hydrogen and carbon is highly endothermic. If mixed with oxygen, however, the combined system of CH_4 and O_2 is unstable, and oxidation to CO_2 and H_2O is exothermic. In this sense, the presence of oxygen "destabilizes" methane, even though the bonding of individual methane molecules is unchanged. Another example is the hydrolysis of saline binary hydrides, e.g., LiH. In isolation, the decomposition of LiH into Li and H_2 is endothermic, but when mixed with water, hydrolysis to LiOH and H_2 is exothermic. In this case, water destabilizes LiH through the formation of LiOH, and the combined system of LiH and H_2O is unstable.

Although the CH_4/O_2 and LiH/H_2O reactions are exothermic and therefore irreversible, smaller changes that lead to shifts in reversible equilibrium reactions are also possible. In particular, the dehydrogenation enthalpy of stable hydrides may be lowered by changing the chemical environment with additives that react during dehydrogenation to form new compounds or alloys [1–3]. The ability to controllably alter the reaction thermodynamics is particularly important in light element (low-Z) metal hydrides that have high thermodynamic stability caused by covalent, polar–covalent, or ionic bonding [4]. Recently, we have used this approach to destabilize low-Z binary [5] and complex hydrides [6]. This has resulted in a decrease in the enthalpy for dehydrogenation and an attendant increase in the equilibrium hydrogen pressure.

The kinetic stability of a chemical system also depends on the chemical environment, but it is not necessarily correlated with the thermodynamic stability. For example, mixtures of methane and oxygen can be kinetically stable if carefully prepared without an ignition source or catalytic surface. In the case of low-Z metal hydrides, the directional nature of the bonding results in high activation energies for atomic diffusion and phase formation kinetics, which leads to prohibitively slow hydrogen exchange rates that are not necessarily increased by thermodynamic destabilization. It is well known that catalytic additives can be used to increase the rates of many types of chemical reactions including hydrogenation and

* Corresponding author. Tel.: +1 310 317 5745.

0925-8388/$ – see front matter © 2007 Elsevier B.V. All rights reserved.
doi:10.1016/j.jallcom.2007.02.080

dehydrogenation in complex hydrides [7–9]. However, because solid-state atomic diffusion is a bulk process and catalysts usually act at surfaces or interfaces, the rate increases possible from catalytic effects alone may be limited. Another way to overcome intrinsically slow diffusion rates in low-Z hydrides is to reduce overall diffusion distances. This may be accomplished by restricting particle or crystallite sizes to the nanometer scale. Reducing particle size also enhances the net reaction rate by increasing surface area and interfacial contact between different phases. There has been considerable effort devoted to producing nanoscale hydride materials using the "top-down" approach of mechanically milling bulk samples [3,10], and more recently, using the "bottom-up" approach of employing nanoporous hosts as particle size-limiting and structure-directing agents [11–13].

In this paper we describe how low-Z binary and complex hydrides can be destabilized using additives that form new compounds during dehydrogenation, and we give several examples from our recent work. We also describe the limitations in the kinetics of these destabilized hydride systems, and we discuss mitigation strategies that employ catalysts and nanoporous scaffolds to improve reaction rates.

2. Destabilization using reactive additives

Fig. 1 shows a general enthalpy diagram illustrating the destabilization of a strongly bound hydride through the addition of a reactive additive. In isolation, the pure hydride AH_2 undergoes dehydrogenation to form $A + H_2$ with a relatively high enthalpy. Consequently, the equilibrium hydrogen pressure will be low. Alternatively, the temperature required for an equilibrium pressure of 1 bar [T (1 bar)], will be high. However, if the chemical environment of AH_2 is altered by adding a second component, B, that alloys with A, then dehydrogenation can proceed to $AB_x + H_2$. This reaction occurs with a reduced enthalpy and, therefore, an increased equilibrium hydrogen pressure. Thus, AH_2 is effectively thermodynamically destabilized, even though the bonding of AH_2 is not altered. This scheme may be contrasted with other approaches where new hydride phases are developed [14–16] or where substitution is used to destabilize the bonding within individual phases [17].

A specific example of the concept illustrated in Fig. 1 is the destabilization of LiH with Si [4,18]. In this case, addition of Si lowers T (1 bar) from >900 to ~490 °C because Li silicides are formed during dehydrogenation. The formation of these compounds reduces the dehydrogenation enthalpy by 70 kJ/mol H_2, which in turn increases the equilibrium hydrogen pressure by up to 10^4 times. Other examples can be interpreted in a similar fashion with this concept; these include the MgH_2/Mg_2Cu [19], $MgH_2/MgAl_x$ [10], $MgH_2/MgCd_x$ [20], TiH_2/Ti_2Cu [21], and LiH/LiAl and $LiH/LiPb_x$ [22] systems. In addition, many new systems have been proposed based on DFT calculations of reaction enthalpies in multi-component systems [23].

3. Equilibrium behavior of the $LiBH_4/MgH_2$ and $LiBH_4/MgX$ destabilized systems

In Fig. 1, the additive, B, does not form a hydride, and destabilization, therefore, occurs with a gravimetric penalty that depends on the relative atomic weights of A and B and the stoichiometry of the AB_x alloy. Using an additive that is itself a hydride can minimize this penalty. An example is the destabilization of $LiBH_4$ with MgH_2 as shown in Fig. 2. Lithium borohydride is a prototypical low-Z complex hydride characterized by ionic bonding between Li^+ cations and covalently bound [BH_4^-] anions [24]. The ionic/covalent bonding in $LiBH_4$ results in high thermodynamic stability. Although T (1 bar) has not been experimentally measured, equilibrium calculations based on established enthalpies, entropies, and heat capacities predict $\Delta H = 67$ kJ/mol H_2 and T (1 bar) = 410 °C for dehydrogenation to $LiH + B + 3/2H_2$ [25]. However, when MgH_2 is present as a destabilizing agent, dehydrogenation can proceed according to:

$$2LiBH_4 + MgH_2 \leftrightarrow 2LiH + MgB_2 + 4H_2. \quad (1)$$

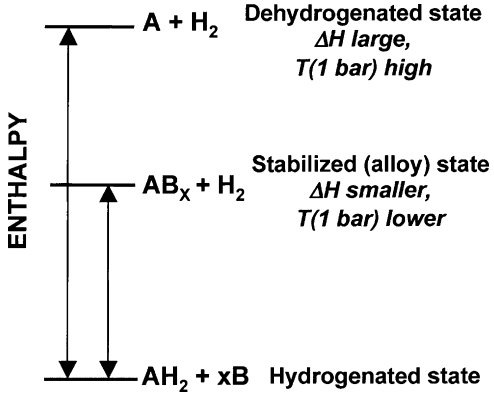

Fig. 1. Generalized enthalpy diagram illustrating destabilization through alloy formation upon dehydrogenation. Including the alloying additive, B, reduces the enthalpy for dehydrogenation through the formation of AB_x and effectively destabilizes the hydride AH_2.

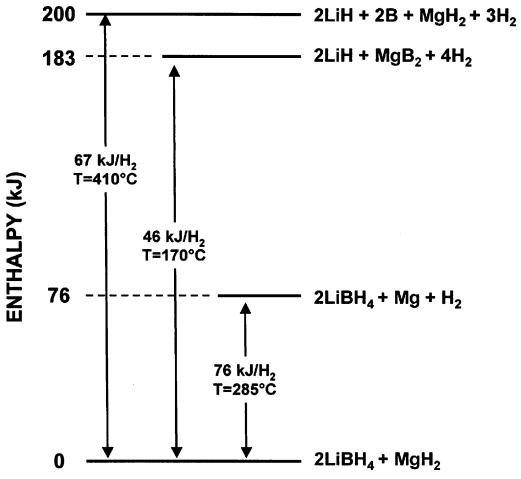

Fig. 2. Enthalpy diagram for the destabilization of $LiBH_4$ by MgH_2. Addition of MgH_2 reduces the enthalpy for dehydrogenation of $LiBH_4$ through the formation of MgB_2. Dehydrogenation of MgH_2 without $LiBH_4$ decomposition is shown as a possible intermediate step.

This reaction has a reduced enthalpy $\Delta H = 46$ kJ/mol H_2 and a calculated T (1 bar) of 170 °C. Formation of MgB_2 upon dehydrogenation, therefore, effectively destabilizes $LiBH_4$.

We have investigated the $LiBH_4/MgH_2$ system experimentally, and found reversible behavior that follows reaction (1) [5]. Beginning with mechanically milled mixtures of either $2LiBH_4 + MgH_2$ or $2LiH + MgB_2$, X-ray diffraction measurements confirmed formation of MgB_2 and LiH upon dehydrogenation and formation of $LiBH_4$ and MgH_2 upon hydrogenation. Volumetric experiments demonstrate the reversible storage of ~10 wt.% hydrogen with no noticeable degradation during five cycles. With isotherms obtained from 315 to 450 °C, the van't Hoff plot shown in Fig. 3 was generated using equilibrium pressures at 4 wt.%. For comparison, Fig. 3 also shows van't Hoff plots for pure $LiBH_4$, calculated using HSC Chemistry [25], and MgH_2, obtained from the IEA/DOE/SNL database [26]. Extrapolating from the measured points, T (1 bar) is estimated to be 225 °C. This value is significantly higher than 170 °C, calculated using HSC for the $LiBH_4/MgH_2$ system. The reason for the discrepancy is unknown; however, the fact that pure $LiBH_4$ melts at ~280 °C is not accounted for in the HSC database. In agreement with the experimental measurements, a T (1 bar) of 225 °C for reaction (1) was recently calculated using DFT calculations with appropriate extensions to finite temperatures [27]. Fig. 3 illustrates that the addition of MgH_2 increases the equilibrium pressure of $LiBH_4$ by approximately 10 times. In addition, for temperatures below 350 °C, the equilibrium pressure for the destabilized system also is higher than the equilibrium pressure for pure MgH_2. In this regime, both $LiBH_4$ and MgH_2 are destabilized by formation of MgB_2 during dehydrogenation.

Other Mg compounds including MgF_2, MgS, and MgSe, can also destabilize $LiBH_4$. Table 1 provides the destabilization reaction, theoretical hydrogen capacity, and calculated T (1 bar) for these systems. We have performed preliminary experimental evaluations of these reactions, and found that mechanically milled mixtures of $2LiF + MgB_2$, $Li_2S + MgB_2$, and $Li_2Se + MgB_2$ all can be hydrogenated at 100 bar hydrogen and 300–350 °C to greater than 75% of the theoretical capacity. The products are $LiBH_4$ and the corresponding MgX compounds. Partial dehydrogenation (greater than 50% of the theoretical capacity) was observed upon heating to 300–450 °C, but the reaction yielded Mg metal in addition to MgB_2, which indicates only partial reversibility. Although reversibility is incomplete, the $LiBH_4/MgH_2$ and $LiBH_4$/MgX systems nonetheless demonstrate that destabilization by additives that react to form new compounds during dehydrogenation is an effective strategy for favorably altering the thermodynamics in complex hydrides.

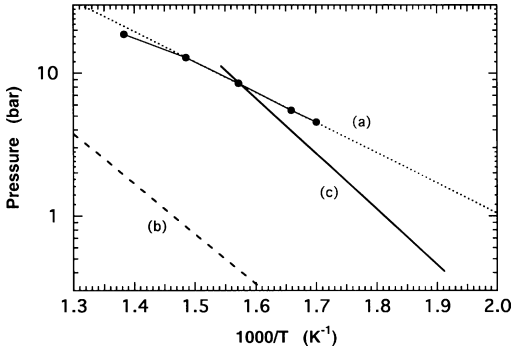

Fig. 3. van't Hoff plots for the $LiBH_4/MgH_2$ destabilized system, $LiBH_4$, and MgH_2. Curve (a) shows equilibrium pressures obtained at 4 wt.% from measured isotherms. Curve (b) shows the calculated behavior for pure $LiBH_4$ [25]. Curve (c) shows the established behavior for MgH_2/Mg [26].

Table 1
$LiBH_4$/MgX destabilized systems

X	Reaction	Capacity (wt.%)	T (1 bar) (°C)[a]
H_2	$2LiBH_4 + MgH_2 \leftrightarrow 2LiH + MgB_2 + 4H_2$	11.6	170
F_2	$2LiBH_4 + MgF_2 \leftrightarrow 2LiF + MgB_2 + 4H_2$	7.6	150
S	$2LiBH_4 + MgS \leftrightarrow Li_2S + MgB_2 + 4H_2$	8.0	170
Se	$2LiBH_4 + MgSe \leftrightarrow Li_2Se + MgB_2 + 4H_2$	5.4	70

[a] T (1 bar) calculated using HSC Chemistry [25].

4. Reaction kinetics in destabilized $LiBH_4$ systems

Measurement of the equilibrium pressures shown in Fig. 3 was hampered by the slow kinetics of the $LiBH_4/MgH_2$ reaction. At temperatures less than ~350 °C, long (~100 h) equilibration times prohibited measurements at temperatures approaching T (1 bar). These limitations in the net reaction rate originate from the kinetics of the individual system components, which are not substantially altered in destabilized systems. Fig. 4 shows the amount of desorbed hydrogen in wt.% (Fig. 4a) and hydrogen pressure (Fig. 4b) for the $LiBH_4/MgH_2$ system and for our preliminary experiments on the $LiBH_4$/MgX systems with X = F_2, S, and Se. Dehydrogenation in the $LiBH_4/MgH_2$ system [curve (H)] occurs in two steps with midpoints at 315 and 410 °C. The first step likely corresponds to dehydrogenation of MgH_2 to Mg metal based on (a) the fact that the desorbed amount, ~2.6 wt.%, is close to the expected amount (2.9 wt.%) for the composition given by reaction (1), and (b) X-ray diffraction measurements on a sample heated only to 350 °C that indicate the presence of Mg metal. The second step corresponds to decomposition of $LiBH_4$ and formation of MgB_2. Thus, the reaction between MgH_2 and $LiBH_4$ is not concerted, but rather proceeds through a $LiBH_4$/Mg intermediate. The enthalpy for this intermediate level is included in Fig. 2. Although the system is destabilized under equilibrium conditions (Fig. 3), the presence of this intermediate indicates that the system it is not kinetically destabilized.

In the $LiBH_4$/MgX systems, which contain only a single hydride component, dehydrogenation occurs over a wide temperature range from 300 to 450 °C without clear evidence of multiple steps. In addition, in spite of the fact that the calculated T (1 bar) varies from 70 to 170 °C for X = F_2, S, and Se, the temperature dependence of hydrogen release during heating is similar for all systems. This result suggests that these systems also are not kinetically destabilized. Further evidence comes from the hydrogen pressures measured during dehy-

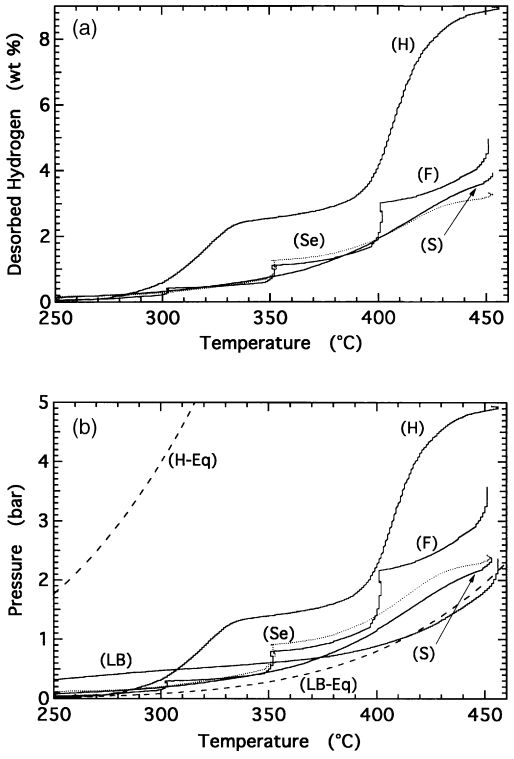

Fig. 4. Hydrogen evolution in $LiBH_4/MgX$, X = H_2, F_2, S, and Se destabilized systems. Panel (a) shows the desorbed hydrogen in wt.% during heating for $2LiBH_4 + MgH_2$ [curve (H)], $2LiBH_4 + MgF_2$ [curve (F)], $2LiBH_4 + MgS$ [curve (S)], and $2LiBH_4 + MgSe$ [curve (Se)]. The heating rate was 2 °C/min. For (F) and (Se), the heating ramp was paused for 1–3 h at 300, 350, and 400 °C. All samples contain 3 mol% $TiCl_3$ as a catalyst. The wt.% hydrogen does not include the catalyst weight. Panel (b) shows the hydrogen pressures for the experiments in panel (a). Panel (b) also shows the hydrogen pressure during heating of pure $LiBH_4$ [curve (LB)], equilibrium pressures calculated for dehydrogenation of $LiBH_4$ to LiH + B [curve (LB-Eq)], and the equilibrium pressure for $LiBH_4/MgH_2$ [curve (H-Eq)] from Fig. 3.

drogenation, which are shown in Fig. 4b for the reactions in Fig. 4a. Also included is the experimentally determined equilibrium hydrogen pressure for reaction (1) extrapolated from the van't Hoff data [curve (H-Eq)] and the measured [curve (LB)] and calculated [curve (LB-Eq)] behavior of pure $LiBH_4$. The separation between curves (H) and (H-Eq) clearly indicates that the $LiBH_4/MgH_2$ system is kinetically limited. At 300 °C dehydrogenation of MgH_2 is just beginning (a hydrogen pressure of ~0.4 bar) yet the equilibrium pressure is ~4 bar. The dehydrogenation of MgH_2 also is not limited by the MgH_2/Mg reaction, which has an equilibrium pressure of hydrogen of 1.8 bar at 300 °C [26]. Similar situations occur for the $LiBH_4/MgX$ systems. Although the equilibrium pressures for these systems have not been measured, the pressures calculated with HSC are all >5 bar at 250 °C. However, during heating, the hydrogen pressures [Fig. 4b, curves (F), (S), and (Se)] are similar to the measured and calculated pressures for pure $LiBH_4$ (~1 bar at 400 °C). For X = F_2 and Se, the temperature ramp was paused for several hours at 300, 350, and 400 °C. During these pauses, the hydrogen pressure rises slowly due to reaction with the destabilizing additive. The results indicate that in all these cases, the kinetics appear to be controlled by $LiBH_4$.

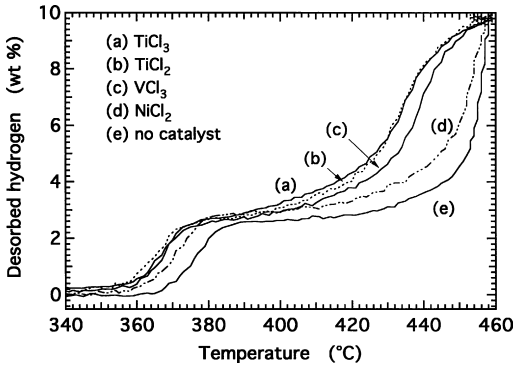

Fig. 5. Effect of catalyst addition on the dehydrogenation of $LiBH_4/MgH_2$. The data show desorbed hydrogen in wt.% during the second dehydrogenation of $2LiBH_4 + MgH_2$ with addition of 3% $TiCl_3$ [curve (a)], 3% $TiCl_2$ [curve (b)], 3% VCl_3 [curve (c)], 3% $NiCl_2$ [curve (d)], and no catalyst [curve (e)]. The wt.% hydrogen does not include the catalyst weight. The heating rate was 3 °C/min. For all of the catalysts shown, the behavior during the first dehydrogenation was nearly identical.

5. Influence of catalytic additives in the $LiBH_4/MgH_2$ system

To realize the full benefit of destabilization, the kinetics must be improved sufficiently to enable operation near T (1 bar). In one approach various catalytic additives to improve the kinetics in the $LiBH_4/MgH_2$ system were evaluated. Several examples are shown in Fig. 5. The best results are obtained with 3% $TiCl_3$. Compared with no additive, the midpoint temperatures for the first and second dehydrogenation steps were lowered by 11 and 22 °C, respectively. Other titanium sources give similar results including $TiCl_2$ (Fig. 5), TiF_3, and $CpTiCl_3$ (Cp = cyclopentadienyl). Addition of 3% VCl_3 or $NiCl_2$ lowers the reaction temperatures for the first step by 9 or 5 °C and the second step by 17 or 5 °C, respectively. The activity with 3% $CrCl_3$ and 3% $NdCl_5$ was similar to that with of 3% VCl_3. Moreover, the addition of pure Ni with a particle size of 50 nm results in reaction temperatures nearly identical to those for 3% $NiCl_2$. For $TiCl_3$ and $CpTiCl_3$, catalyst loadings of approximately 3 mol% are optimal, while higher loadings (>9%) lead to similar reaction temperatures but reduced capacities. Although transition metal additives introduced as halides or nanoparticles do indeed reduce the reaction temperatures in this system, the best catalysts all behave similarly and dehydrogenation still occurs in two steps at temperatures >300 °C. These results suggest that the catalysts may be enhancing one rate-limiting step, but other step(s) still prohibit a concerted reaction. One possibility is that the catalysts are improving the rate of hydrogen exchange with the gas phase but the rate of diffusion within the hydride phases remains slow. Further study to understand the catalytic mechanisms will hopefully lead to additional kinetic improvements.

6. Kinetics of destabilized hydrides incorporated in nanoporous scaffolds

Another way to improve the rates of hydrogen exchange in low-Z complex and destabilized hydrides is to use reduced par-

ticle sizes. Mechanical milling has been extensively studied [3], and although this technique does not lead to particularly small individual particle sizes (typically 1–10 μm), the extreme deformation during high energy milling can lead to intra-particle crystallite sizes of less than 100 nm. Together with large intergranular volumes, the presence of these small crystallites can improve diffusion rates, and therefore enhance the rates of hydrogen exchange.

A different approach to reducing and limiting particle size is to use nanoporous host scaffolds. Hydride materials incorporated into these hosts will have particle dimensions limited by the available pore size. Although the intrinsic diffusion rates may not change with this approach, the reduced diffusion distances should increase the overall rates of hydrogen exchange. An additional advantage of host scaffolds is that the sintering of particles during cycling can be inhibited.

To evaluate the influence of nanoporous scaffolds on hydrogen exchange kinetics we conducted initial studies with pure $LiBH_4$ contained within nanoporous carbon aerogels. This hydride was chosen because its bulk dehydrogenation kinetics are slow, its reversibility is poor, and it is a common component in destabilized systems. Carbon aerogels were chosen because they are expected to be relatively chemically inert. Fig. 6 shows data from temperature ramp experiments for the dehydrogenation of $LiBH_4$ contained within an aerogel with an average pore size of 13 nm and for a control sample of $LiBH_4$ mixed with nonporous graphite. The weight fraction of $LiBH_4$ in both the aerogel and the control sample was 28 wt.%. Additional experimental details, including the synthesis and characterization of the aerogel and techniques for incorporating $LiBH_4$, will be provided elsewhere [28]. Upon heating, the dehydrogenation of the control sample begins at 285 °C (when $LiBH_4$ melts), although after 2 h at 300 °C, less than 0.3 wt.% hydrogen is desorbed. In contrast, the dehydrogenation of $LiBH_4$ contained within the aerogel begins at ~240 °C and reaches 1.9 wt.% hydrogen desorption after 2 h at 300 °C. Thus, the incorporation of $LiBH_4$ into the aerogel increases the extent of its dehydrogenation at 300 °C approximately seven-fold. At 400 °C, 3.7 wt.% hydrogen is desorbed from the aerogel sample. Accounting for the weight of the aerogel, this amount of hydrogen corresponds to nearly complete (>95%) dehydrogenation of the $LiBH_4$ into LiH + B. In contrast, the extent of dehydrogenation in the control sample is only 70% after heating to 400 °C. In this example, the results indicate that the incorporation of a complex hydride material into a nanoporous host can significantly improve dehydrogenation kinetics.

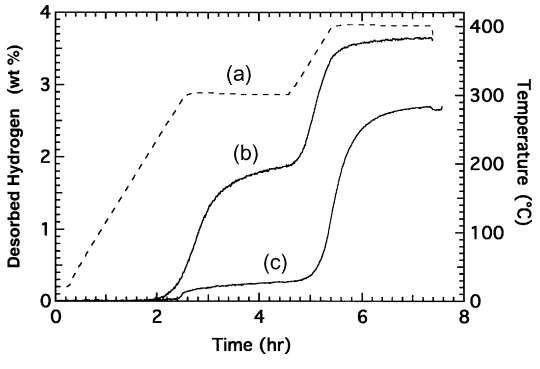

Fig. 6. Dehydrogenation of $LiBH_4$ in a nanoporous carbon aerogel. Curve (a) shows the temperature profile (right axis). Curve (b) shows the hydrogen evolution in wt.% (left axis) for $LiBH_4$ incorporated into a 13 nm average pore size carbon aerogel. The loading of $LiBH_4$ in the aerogel was 28 wt.%. Curve (c) shows hydrogen evolution from a control sample consisting of 28 wt.% $LiBH_4$ mixed with 72 wt.% nonporous graphite. The wt.% hydrogen includes the weights of both the $LiBH_4$ and the carbon.

The reversibility of $LiBH_4$ in the aerogel was also examined. After dehydrogenation as shown in Fig. 6, the samples were rehydrogenated by heating at 400 °C for 2 h in 100 bar hydrogen to complete one dehydrogenation/rehydrogenation cycle. After a second (identical) cycle, a third dehydrogenation was performed. Compared to the initial extent of dehydrogenation (>95% for the aerogel sample and 70% for the control), the final capacities were significantly lower (55% for the aerogel and 20% for the control samples). Although significant degradation occurred in both samples, the degradation was less for $LiBH_4$ contained in the aerogel. This improved cycling capacity likely is related to the constrained LiH and B particle sizes forming within the aerogel. The limited particle sizes also likely increase the contact area between LiH and B phases, which can further improve the kinetics of the rehydrogenation reaction.

In these experiments, the pore volume of the aerogel was 0.8 cm^3/g. This volume permits maximum $LiBH_4$ loadings of only about 30 wt.%. To minimize the weight penalty from the scaffold for practical applications, we estimate that loadings of at least 70 wt.% will be necessary, which may be achieved with aerogel pore volumes of 3–4 cm^3/g. Such large volumes are known to exist for several porous host materials (e.g., silica), although it has not yet been established that these materials will yield similar improvements.

7. Summary

We have shown that the thermodynamic properties of light element hydrides can be altered using additives that form new phases upon dehydrogenation. These additives modify the chemical environment of strongly bound hydrides by creating new reaction pathways without directly perturbing the bonding within individual phases. This strategy has been used to develop several destabilized systems based on $LiBH_4$. For the $LiBH_4/MgH_2$ system, reversible storage of approximately 10 wt.% has been achieved with an equilibrium hydrogen pressure ~10 times greater than the pressure for pure $LiBH_4$. In addition, partial reversibility has been observed for $LiBH_4$ destabilized by MgF_2, MgS, and MgSe.

All of these systems exhibit rates of hydrogen exchange that are much too slow for practical applications. This issue is especially acute for destabilized systems that have increased equilibrium pressures, and therefore, ideally operate at lower temperatures. We have also shown that the hydrogen exchange kinetics appear to be controlled by the kinetics of pure $LiBH_4$ and are not affected by the destabilizing additive.

Improvements to the kinetics have been made with catalytic additives based on transition metals, although the resulting rates are still too slow. The kinetics also can be improved by

reducing particle sizes to the nanometer scale, which reduces overall reaction times by reducing diffusion distances. Following this approach, we have shown that $LiBH_4$ incorporated into a nanoporous carbon aerogel exhibits significantly enhanced rates of dehydrogenation and improved reversibility.

The use of reactive additives to destabilize light element hydride systems appears to be a promising and versatile approach for achieving a hydrogen storage material with the required equilibrium properties for practical applications. We can improve the kinetics of these destabilized systems by catalysis and nanoscale engineering, but reaching the necessary rates of hydrogen exchange remains a significant challenge.

Acknowledgements

The authors gratefully acknowledge the U.S. Department of Energy for partial support of this work (DOE contract DE-FC36-05GO15067).

References

[1] R. Wiswall, in: G. Alefeld, J. Völkl (Eds.), Hydrogen in Metals II, Springer-Verlag, Berlin, 1978, pp. 201–242.
[2] R. Griessen, T. Riesterer, In: Hydrogen in Intermetallic Compounds, Springer-Verlag, Berlin, 1988, pp. 219–284.
[3] J. Huot, in: H.S. Nalwa (Ed.), Nanoclusters and Nanocrystals, American Scientific Publishers, New York, 2003, pp. 53–85.
[4] E. Wiberg, E. Amberger, Hydrides of the Elements of Main Groups I–IV, Elsevier, Amsterdam, 1971.
[5] J.J. Vajo, F. Mertens, C.C. Ahn, R.C. Bowman Jr., B. Fultz, J. Phys. Chem. B 108 (2004) 13977–13983.
[6] J.J. Vajo, S.L. Skeith, F. Mertens, J. Phys. Chem. B 109 (2005) 3719–3722.
[7] B. Bogdanović, M. Schwickardi, J. Alloys Compd. 253–254 (1997) 1.
[8] C.M. Jensen, K.J. Gross, Appl. Phys. A 72 (2001) 213–219.
[9] F. Schüth, B. Bogdanović, M. Felderhoff, Chem. Commun. (2004) 2249–2258.
[10] A. Zaluska, L. Zaluski, J.O. Ström-Olsen, Appl. Phys. A 72 (2001) 157–165.
[11] A. Gutowska, L. Li, Y. Shin, C.M. Wang, X.S. Li, J.C. Linehan, R.S. Smith, B.D. Kay, B. Schmid, W. Shaw, M. Gutowski, T. Autrey, Angew. Chem. Int. Ed. 44 (2005) 3578–3582.
[12] F. Schüth, B. Bogdanović, A. Taguchi, Patent application WO2005014469.
[13] C.P. Baldé, B.P.C. Hereijgers, J.H. Bitter, K.P. de Jong, Angew. Chem. Int. Ed. 45 (2006) 3501–3505.
[14] J. Graetz, Y. Lee, J.J. Reilly, S. Park, T. Vogt, Phys. Rev. B 71 (2005) 184115.
[15] F.E. Pinkerton, G.P. Meisner, M.S. Meyer, M.P. Balogh, M.D. Kundrat, J. Phys. Chem. B 109 (2005) 6–8.
[16] W. Grochala, P.P. Edwards, Chem. Rev. 104 (2004) 1283–1315.
[17] Y. Nakamori, S. Orimo, J. Alloys Compd. 370 (2004) 271–275.
[18] R.C. Bowman Jr., S.-J. Hwang, C.C. Ahn, J.J. Vajo, Mater. Res. Soc. Symp. Proc. 837 (2005), N3.6.1–N3.6.6.
[19] J.J. Reilly, R.H. Wiswall, Inorg. Chem. 6 (1967) 2220–2223.
[20] G. Liang, R. Schulz, J. Mater. Sci. 39 (2004) 1557–1562.
[21] A.J. Maeland, J. Less Common Met. 89 (1983) 173.
[22] E. Veleckis, J. Less Common Met. 73 (1980) 49–60.
[23] S.V. Alapati, J.K. Johnson, D.S. Sholl, J. Phys. Chem. B 110 (2006) 8769–8776.
[24] K. Miwa, N. Ohba, S. Towata, Y. Nakamori, S. Orimo, Phys. Rev. B 69 (2004) 245120.
[25] Outokumpu HSC Chemistry for Windows, version 4.0, ChemSW, Inc., 1999.
[26] G. Sandrock, G. Thomas, Appl. Phys. A 72 (2001) 153–155.
[27] N.A. Zarevich, S.V. Alapati, D.D. Johnson, J. Phys. Chem. B, submitted.
[28] A.G. Gross, J.J. Vajo, S.L. Skeith, G.L. Olson, in preparation.